Progress In Electromagnetics Research B, Vol. 90, 187–205, 2021

An Overview of Rainfall Fading Prediction Models for Satellite Links in Southern Africa

Djuma Sumbiri* **and Thomas J. O. Afullo**

Abstract—This work presents an overview of rainfall fading models over satellite links in South Africa using three years of rainfall data collected by the Joss-Waldvogel RD-80 disdrometer in Durban, South Africa (29° 52′S, 30° 58′E), alongside a colocated Ku-band satellite TV link. Different drop size distribution models, such as Lognormal, Gamma, Weibull, and the Optimised drop size distribution model for Equatorial Africa, are used to formulate the rainfall attenuation models used in this study. Thereafter, the formulated attenuation models are used to convert rainfall rate time series data to predicted rainfall attenuation time series. In addition, both the ITU-R model and the Synthetic Storm Techniques are applied for comparison with the above rainfall attenuation models alongside experimental measurements over the 12.6 GHz satellite TV link from Intelsat-20 (IS-20) located at 68.5°E on the azimuth angle of 57.5° with respect to Durban.

1. INTRODUCTION

For satellite communication systems operating above 10 GHz, rainfall is a major propagation impairment affecting the delivery of services due to the attenuation and degradation of the received signal during transmission [1, 2]. That is why numerical and empirical prediction techniques have been developed in different parts of the world to estimate the attenuation due to rain in order to minimize fading outage over such links. In some parts of the world, owing to the lack of real attenuation data, this is generated by rainfall rate time series at any frequency and polarization. In this paper, we use the rainfall measurement in Durban, South Africa, to provide a reliable prediction of rainfall attenuation on the received signal for the Intersat-20 12.6 GHz satellite TV link located at 68.5°E on the elevation angle of 36.5°. We employ the Synthetic Storm Technique (SST), the International Telecommunication Union-Recommendation (ITU-R) model, and other established statistical models such as Lognormal (LGN), Gamma (GM), and the Weibull (WBL) distributions. Three years of rainfall data were collected from 2014 to 2016 using the Joss-Waldvogel RD-80 disdrometer installed on the rooftop of the Electrical Engineering Building, University of Kwa-Zulu Natal, Howard College, Durban in South Africa (29° 52′S, 30° 58′E) — which is colocated with the satellite link. Predicted rainfall attenuation time series is validated with the colocated satellite link measurement data.

The present submission is a follow-up to earlier publications pertaining to rain attenuation and raindrop size distribution modelling in the sub-Tropical Africa, including Southern Africa and Equatorial Africa regions. These included the works of Afullo [3], Akuon and Afullo [4], Alonge and Afullo [5], Adetan and Afullo [6], and more recent publications by Sumbiri et al. [7], Afolayan et al. [8], Ahuna et al. [9]. Further, we have the recent submissions by Ahuna et al. on the rainstorm characterization [11], and the latest modified raindrop size modelling approach by Alonge [12], and the optimized raindrop size distribution by Sumbiri and Afullo [18]. Thus, we are furthering the effort to improve rain attenuation

Received 24 November 2020, Accepted 28 January 2021, Scheduled 13 February 2021
* Corresponding author: Djuma Sumbiri (sumbirdj@gmail.com).
The authors are with the Discipline of Electrical, Electronic & Computer Engineering, School of Engineering, University of Kwa-Zulu Natal (UKZN), Durban 4041, South Africa.

modelling in sub-Saharan Africa. The rest of the paper is organized as follows: Section 2 focuses on the experimental data; Section 3 presents the attenuation prediction models; Section 4 presents the results and discussions; and finally, Section 5 gives the conclusions.

2. LOCATION AND PROPAGATION EXPERIMENTAL DATA

Propagation measurements over a vertically polarized Ku-band satellite signal level from Intelsat-20 (IS-20) located at 68.5°E on the azimuth angle of 57.5° with respect to Durban were undertaken on the rooftop of the Electrical Engineering building (29° 52′S, 30° 58′E), University of Kwa-Zulu Natal, Howard College, Durban in South Africa since 2012. A Ku-band, 12.6 GHz of 8-PSK (8-*ary* Phase Shift Keying) signal is received by a 90 cm offset parabolic antenna dish at an elevation angle of 36.5°. The Rhode and Schwarz FSH8 spectrum analyser monitors and captures the received signal level (RSL) over the link. The RSL measurements are recorded with logging data in one-minute sampling period and stored in a computer. The link budget of this satellite link is detailed in Table 1.

Table 1. Link budget [4].

STAGE	LINK	GAINS (dB)	LOSSES (dB)
	EIRP (dBm)	85	
Satellite Antenna Downlink Transmission	Receive Antenna gain (dBi)	40	
	LNB gain	55	
	Peripheral Cable Loss		3
	Atmospheric Loss		2
	Free Space Loss		206
	Offset/Contour Loss		3
	Splitter Loss		7
	RF Attenuation at Spectrum Analyser		20
	TOTAL	180	241
	Received Power Level	≈ −61 dBm	
Post-Antenna Processing	Noise Floor (at 40 MHz bandwidth)	−97 dBm	
	5/6 8-*ary* PSK C/N Margin	25 dB	
	LNB Noise Figure	0.3 dB	
	Receiver Sensitivity (dBm)	≈ −71.7 dBm	

Furthermore, three years of rainfall rate and drop size distribution measurement at 30-second integration time was collected over a period of three years (2014 to 2016) using the Joss-Waldvogel RD-80 disdrometer installed such that its rainfall sensor was set close to the receiver satellite antenna. The collected rainfall measurement was converted to one-minute integration time using the relationship obtained by Mary and Ahuna et al. in [9]:

$$R_{30S} = 1.051\,(R_{1,DBN})^{1.004} \tag{1}$$

where R_{30S} is the rainfall rate in mm/h at 30-second integration time, and $R_{1,DBN}$ is the rainfall rate at one-minute integration time in Durban.

From Table 1, the expected power at the receiver is −61 dBm, with receiver sensitivity of −71.7 dBm. This means that the clear-air signal remains 10.7 dB above the squelch level, and this can only be guaranteed for rain rates up to about 50 mm/h — since beyond this rainfall rate, the satellite receiver squelches. Measured data are generated by the following power law relationship obtained by Afolayan et al. using rainfall drops for the 12.6 GHz satellite TV link RSLlevel observed during rainy periods [8]:

$$A_{av} = 1.3387R^{0.5482} \tag{2}$$

The in-depth measurement process for this 12.6 GHz satellite TV link in Durban is detailed in [10].

3. ATTENUATION PREDICTION MODELS

In this section, the ITU-R model, Synthetic Storm Technique, several established DSD models (Lognormal model [13, 14], Gamma model [15], Weibull model [16, 17]), and the Optimised drop size distribution model for Equatorial Africa [18] are used to estimate the rainfall attenuation used in this paper.

3.1. ITU-R Rain Attenuation Model

The ITU-R Recommendation P.618-13 [19] provides a simple method to estimate the statistical rainfall attenuation on a slant (earth-space) path at a given location. This method employs some parameters of the link and its location as inputs into the attenuation prediction process as illustrated in Figure 1.

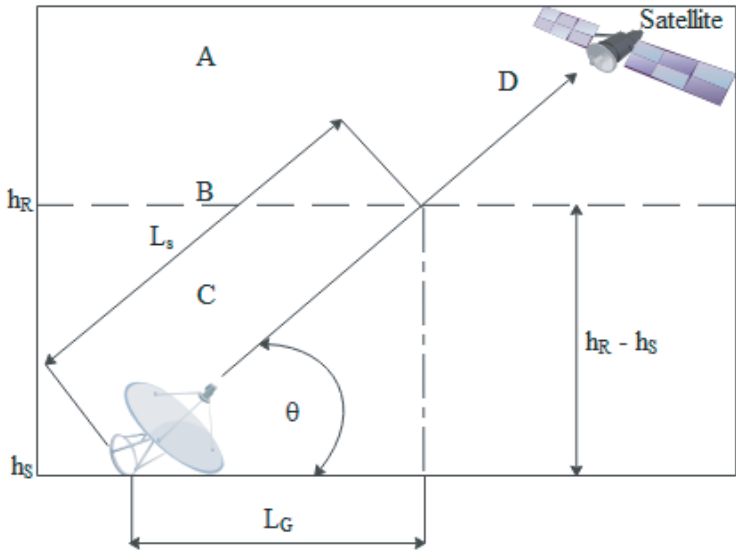

Figure 1. Schematic diagram of an Earth-space path.

From Figure 1 (as also observed in the presentation by Freeman [22]), region A represents the frozen precipitation zone; line B, the rain height; region C, the region of liquid precipitation; and region D, the Earth space path. For elevation angle $\theta \geq 5°$, the slant path length, L_S, is expressed by [19]:

$$L_s = \frac{(h_R - h_s)}{\sin\theta}\,\text{km} \tag{3}$$

For $\theta \leq 5°$, the slant path length is given by the following expression [19]:

$$L_s = \frac{2\,(h_R - h_s)}{\left(\sin^2\theta + \dfrac{2\,(h_R - h_s)}{R_e}\right)^{1/2} + \sin\theta}\,\text{km} \tag{4}$$

where $R_e = 8500\,\text{km}$ is the effective radius of the earth, $h_S\,(\text{km})$ the height of the earth station above sea level, and $h_R\,(\text{km})$ the rain height given by the following expression [20]:

$$h_R = h_o + 0.36\,\text{km} \tag{5}$$

According to ITU-R model, the rainfall specific attenuation $A_S\,(\text{dB/km})$ can be determined from the rainfall rate $R\,(\text{mm/h})$ using the following power law expression [21–23]:

$$A_S = kR^{\alpha}\,\text{dB/km} \tag{6}$$

where k and α are the power-law coefficients depending on frequency of transmission accessible in ITU-R P.838-3 [15]. The total predicted path attenuation $A\,(\mathrm{dB})$ is obtained from:

$$A = A_S \cdot L_E \,\mathrm{dB} \tag{7}$$

where L_E is the effective path length obtained as follows [19]:

- Calculate the horizontal reduction factor, $r_{0.01}$:

$$r_{0.01} = \frac{1}{1 + 0.78 - \sqrt{\dfrac{L_G A_S}{f}} 0.38\,(1 - e^{-2L_G})} \tag{8}$$

where L_G is the horizontal projection of the slant-path as shown in Figure 1 and is given by the following expression:

$$L_G = L_S \cos\theta \,\mathrm{km} \tag{9}$$

- Then, calculate the vertical adjustment factor, $\upsilon_{0.01}$:

$$\xi = \tan^{-1}\left(\frac{h_R - h_S}{L_G r_{0.01}}\right) \text{ degrees} \tag{10}$$

For $\xi > \theta$, $L_R = \frac{L_G r_{0.01}}{\cos\theta}$ km
Else, $L_R = \frac{(h_R - h_s)}{\sin\theta}$ km
If $|\varphi| < 36°$, $\chi = 36 - |\varphi|$ degrees

$$\upsilon_{0.01} = \frac{1}{1 + \sqrt{\sin\theta}\left(31\left(1 - e^{-(1/(1+x))}\right)\dfrac{\sqrt{L_R A_S}}{f^2} - 0.45\right)} \tag{11}$$

- The effective path length L_E is given by the following expression:

$$L_E = L_R \upsilon_{0.01} \,\mathrm{km} \tag{12}$$

The basic parameters for the satellite link are presented in Table 2.

Table 2. Basic link parameters.

Parameter	Value
Elevation Angle (θ)	36.5°
Total distance to satellite	38,050 km
Longitudinal position of Satellite	68.5°
Ground azimuth of satellite	57.5°
Height above sea level (a.s.l) (h_S)	0.176 km
Rain Height (h_R)	4.96 km
Slant Path Length (L_S)	8.042 km
Beacon Central Frequency	12.6 GHz
Total bandwidth	40 MHz

3.2. The Synthetic Storm Technique

The Synthetic Storm Technique (SST) was developed by Drufuca [24] and refined by Matricciani [1, 26, 30] to predict the rainfall attenuation for both terrestrial and slant path earth-space links for different frequencies and polarisations in the absence of real attenuation data [25–29]. This approach consists of converting a rain rate time series measured by a disdrometer or a rain gauge at any geographical location into a rainfall attenuation time series [30]. The model requires the knowledge about the length of the signal path between the satellite and the base station $L\,(km)$, the rainfall cell speed (v), and the rainfall rate time series measured at the location under investigation. The physical fundamentals and mathematical concepts of this model are detailed in [30]. The vertical structure of rainfall is modelled with two different layers, specifically, the rain layer A (raindrops at 20°C) and the melting layer B (melting hydrometeors at 0°C) as shown in Figure 2. The rainfall rate R_B (apparent rainfall rate) in layer B is related to the rainfall rate $R_A = R$, in the layer A by the following Expression [30]:

$$R_B = rR, \quad \text{with} \quad r = 3.134 \tag{13}$$

The total predicted link attenuation A (dB) can be calculated as [30]:

$$A(x) = K_A \int_0^{L_A} R^{\alpha_A}(x_o + \Delta x_o, \xi)\, d\xi + K_B r^{\alpha_B} \int_{L_A}^{L_B} R^{\alpha_B}(x_o, \xi)\, d\xi \tag{14}$$

where $A(x)$ is the rainfall attenuation at a specific point along the link length $L\,(km)$, ξ, the distance measured along the satellite link. Constant values k and α are dependent on frequency and polarisation of the electromagnetic wave. They are available in ITU-R P.838-3 for water temperature of 20°C [21] and in [31] for water of 0°C.

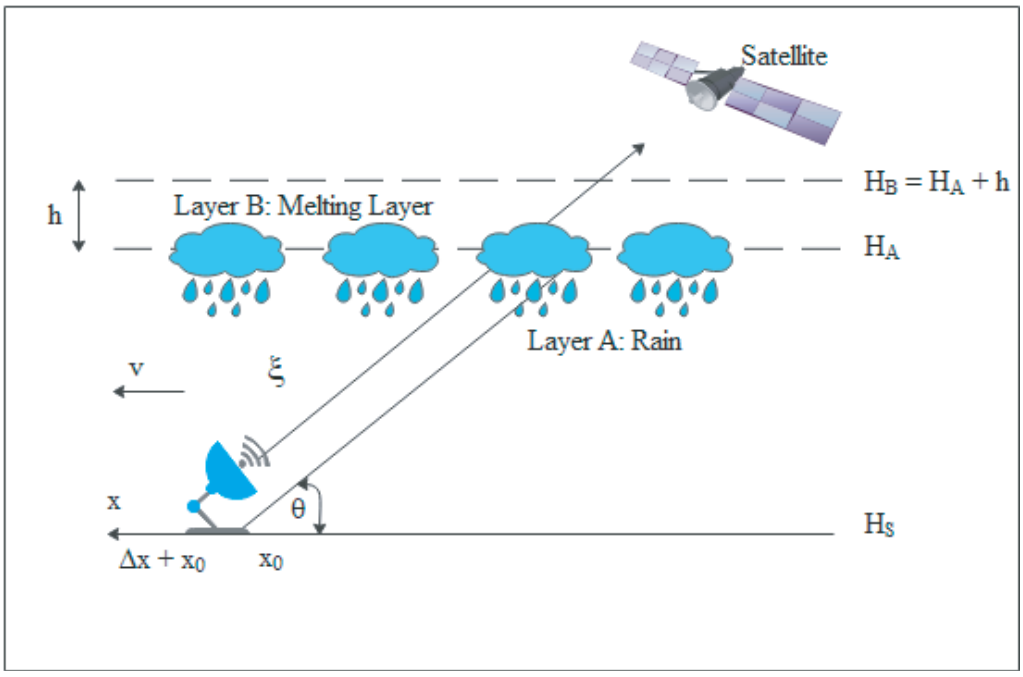

Figure 2. Vertical structure of rainfall for Synthetic Storm Technique [26, 30].

The rainy paths, L_A and L_B,j are obtained from [30]:

$$L_A = \frac{H_A - H_S}{\sin\theta} \tag{15}$$

$$L_B = \frac{H_B - H_S}{\sin\theta} \tag{16}$$

where H_S (km) is the height of the earth station above sea level, and H_A (km) and H_B (km) are heights above sea level for the upper limits of layer A and layer B, respectively. According to [20], the upper limit of layer B is given by:

$$H_B = h_0 + 0.36 \tag{17}$$

where h_o is the mean 0°C isotherm height above sea level (a.s.l.) The height above sea level for the upper limit of layer A is given by:

$$H_A(\varphi) = H_B(\varphi) - h \tag{18}$$

Here $h = 0.4$ km is the depth of layer B taken by assumption irrespective of the latitude.

By applying Fourier Transform and making some assumptions in Eq. (13), Matricciani [30] has derived the following expression for calculating the satellite link signal attenuation due to rainfall:

$$A(t) = K_A R^{\alpha_A}(t) L_A + r^{\alpha_B} K_B R^{\alpha_B}(t) (L_B - L_A) \tag{19}$$

Table 3 presents the two layers' parameters for vertical structure of precipitation using the Synthetic Storm Technique.

Table 3. Parameters used for vertical structure of rainfall using SST [8, 10].

Parameter	Layer A (Rain layer)	Layer B (Melting layer)
k	0.02421	0.0168
α	1.1516	1.26
H	4.6 km	4.96 km
L	7.43778 km	8.043 km
Elevation angle	36.5°	
Storm speed	9.41 m/s	
frequency	12.6 GHz	

3.3. Lognormal Rain Attenuation Model

This model is formulated from the lognormal raindrop size distribution model (LGN) as given in [13, 14] for all rainfall regimes. The total predicted path attenuation A (dB) can be expressed as:

$$A\ (\text{dB}) = A_S L_E \tag{20}$$

where A_S is the specific attenuation due to rainfall drops and is expressed by the following expression [32–35]:

$$A_S\ [\text{dB/km}] = 4.343 \times 10^{-3} \int_0^\infty Q_{ext}(D) N(D) dD \tag{21}$$

Here, $N(D)$ is the raindrop size distribution, $N(D)dD$ the density number of the drop with diameter D (mm) in the diameter dD interval, and Q_{ext} (mm^2) the extinction cross-section determined from Mie scattering theory for frequencies above 3 GHz [35].

From the Joss-Waldvogen disdrometer channels, Equation (19) is rewritten as follows [37]:

$$A\ (\text{dB}) = \left[4.343 \times 10^{-3} \sum_{i=1}^{20} k_{ext} \bar{a}^{\varsigma_{ext}} N(D_i) \Delta D_i \right] \cdot L_E \tag{22}$$

where $N(D_i)$ is the drop size distribution model, $Q_{ext} = k_{ext} \bar{a}^{\varsigma_{ext}}$, expressed as power law expression as function of D (mm), where $\overline{a} = \frac{D}{2}$ is the radius of the rain drop (here assumed spherical); k_{ext} and ς_{ext} are both frequency and temperature dependent coefficients derived using Mie scattering technique [37].

The Lognormal rainfall drop size distribution model is given by [13, 14]:

$$N(D_i) = \frac{N_T}{\sigma D_i \sqrt{2\pi}} \exp\left\{ -\frac{1}{2} \left[\frac{\ln(D_i) - \mu}{\sigma} \right]^2 \right\} \tag{23}$$

Substituting Equation (22) into Equation (21), we have:

$$A\ (\text{dB}) = \left[4.343 \times 10^{-3} \sum_{i=1}^{20} k_{ext} \bar{a}^{\varsigma_{ext}} \cdot \frac{N_T}{\sigma D_i \sqrt{2\pi}} \exp\left\{-\frac{1}{2}\left[\frac{\ln(D_i) - \mu}{\sigma}\right]^2\right\} \Delta D_i\right] \cdot L_E \tag{24}$$

The expression between square brackets in Eq. (23) represents the rainfall specific attenuation, and it is rewritten as the power law expression below:

$$A_S = 4.343 \times 10^{-3} \sum_{i=1}^{20} k_{ext} \bar{a}^{\varsigma_{ext}} \cdot \frac{N_T}{\sigma D_i \sqrt{2\pi}} \exp\left\{-\frac{1}{2}\left[\frac{\ln(D_i) - \mu}{\sigma}\right]^2\right\} \Delta D_i = k_{LGN} R^{\alpha_{LGN}} \tag{25}$$

Substituting Equation (24) into (23), the total predicted path attenuation with the Lognormal distribution model is given by:

$$A\ (\text{dB}) = k_{LGN} R^{\alpha_{LGN}} \cdot L_E \tag{26}$$

where L_E is the effective path length as described in (11); R is the rainfall rate in (mm/h); k_{LGN} and α_{LGN} are lognormal regression coefficients depending on the frequency of transmission.

3.4. The Modified Gamma Rain Attenuation Model

This model is formulated based on the Modified Gamma Model (GM) as given in [16]. The Modified Gamma raindrop size distribution model is thus given by:

$$N(D_i) = N_m (D_i)^{\mu} \exp(-\Lambda D_i) \tag{27}$$

Substituting Eq. (26) into Eq. (21), we have:

$$A\ (\text{dB}) = \left[4.343 \times 10^{-3} \sum_{i=1}^{20} k_{ext} \bar{a}^{\varsigma_{ext}} \cdot N_m (D_i)^{\mu} \exp(-\Lambda D_i) \Delta D_i\right] \cdot L_E \tag{28}$$

where the expression between square brackets in Eq. (27) represents the rainfall specific attenuation, and it is rewritten as the power law expression below:

$$A_S = 4.343 \times 10^{-3} \sum_{i=1}^{20} k_{ext} \bar{a}^{\varsigma_{ext}} \cdot N_m (D_i)^{\mu} \exp(-\Lambda D_i) \Delta D_i = k_{GM} R^{\alpha_{GM}} \tag{29}$$

Substituting Equation (28) into (27), the total predicted path attenuation due to rain with a modified Gamma distribution is given by:

$$A\ (\text{dB}) = k_{GM} R^{\alpha_{GM}} \cdot L_E \tag{30}$$

where L_E is the effective path length as described in Eq. (11); R is the rainfall rate in (mm/h); k_{GM} and α_{GM} are modified gamma regression coefficients depending on the frequency of transmission.

3.5. The Weibull Rain Attenuation Model

This model is formulated based on the Weibull distribution (WBL) as presented in [16, 17]. The Weibull rainfall drop size distribution model is given by:

$$N(D_i) = N_w \left(\frac{\beta}{\gamma}\right) \left(\frac{D_i}{\gamma}\right)^{\beta-1} \exp\left[-\left(\frac{D_i}{\gamma}\right)^{\beta}\right] \tag{31}$$

Substituting Eq. (30) into Eq. (21), we have:

$$A\ (\text{dB}) = \left[4.343 \times 10^{-3} \sum_{i=1}^{20} k_{ext} \bar{a}^{\varsigma_{ext}} \cdot N_w \left(\frac{\beta}{\gamma}\right) \left(\frac{D_i}{\gamma}\right)^{\beta-1} \exp\left[-\left(\frac{D_i}{\gamma}\right)^{\beta}\right] \Delta D_i\right] \cdot L_E \tag{32}$$

where the expression between square brackets in Eq. (31) represents the rainfall specific attenuation, and it is also rewritten as the power law expression below:

$$A_S = 4.343 \times 10^{-3} \sum_{i=1}^{20} k_{ext} \bar{a}^{\varsigma_{ext}} \cdot N_w \left(\frac{\beta}{\gamma}\right) \left(\frac{D_i}{\gamma}\right)^{\beta-1} \exp\left[-\left(\frac{D_i}{\gamma}\right)^{\beta}\right] \Delta D_i = k_{WBL} R^{\alpha_{WBL}} \tag{33}$$

Substituting Eq. (32) into Eq. (31), the total predicted path attenuation due to rain with a Weibull distribution is given by:

$$A \text{ (dB)} = k_{WBL} R^{\alpha_{WBL}} \cdot L_E \tag{34}$$

Here L_E is the effective path length as described in Eq. (11); R is the rainfall rate in (mm/h); k_{WBL} and α_{WBL} are Weibull regression coefficients depending on the frequency of transmission. Table 4 presents values of coefficients k and α for LGN, GM, and WBL models as given in [36].

Table 4. Coefficients k and α for different models, Durban at 20°C [36].

Frequency (GHz)	LGN Model		GM Model		WBL Model	
12.6	k	α	k	α	k	α
	0.017	1.097	0.0174	1.095	0.0129	1.290

3.6. The Optimized Rain Drop Size Distribution Model for Equatorial Africa

This is a new "Optimized" rainfall DSD model developed by Sumbiri and Afullo using rainfall measurement undertaken in Butare, Rwanda, Central Africa [18]. This model is given by the following expression [18]:

$$N(D_i) = \frac{N_T}{C\sigma D_i \sqrt{2\pi}} \exp\left\{-\frac{1}{2}\left[\frac{ln(D_i) - \mu}{\sigma}\right]^2\right\} \{1 + \alpha \exp(-(D_i)\} \tag{35}$$

Substituting Eq. (34) into Eq. (21), we have:

$$A \text{ (dB)} = \left[4.343 \times 10^{-3} \sum_{i=1}^{20} k_{ext} \bar{a}^{\varsigma_{ext}} \frac{N_T}{C\sigma D_i \sqrt{2\pi}} \exp\left\{-\frac{1}{2}\left[\frac{\ln(D_i) - \mu}{\sigma}\right]^2\right\} \{1 + \alpha \exp(-(D_i)\} \Delta D_i\right] \cdot L_E \tag{36}$$

where the expression between square brackets in Eq. (35) represents the rainfall specific attenuation, and it is, again, rewritten as the power law expression below:

$$4.343 \times 10^{-3} \sum_{i=1}^{20} k_{ext} \bar{a}^{\varsigma_{ext}} \frac{N_T}{C\sigma D_i \sqrt{2\pi}} \exp\left\{-\frac{1}{2}\left[\frac{\ln(D_i) - \mu}{\sigma}\right]^2\right\} \{1 + \alpha \exp(-(D_i)\} \Delta D_i = k_{Opt} R^{\alpha_{Opt}} \tag{37}$$

Substitution of Equation (36) into Equation (35), the total predicted path attenuation due to rain with the proposed distribution can be calculated as follows:

$$A \text{ (dB)} = k_{Opt} R^{\alpha_{Opt}} \cdot L_E \tag{38}$$

where L_E is the effective path length as described in Eq. (11); R is the rainfall rate in (mm/h); coefficients k_{Opt} and α_{Opt} are equal to 0.0212 and 1.1091 respectively at 12.6 GHz [37].

4. RESULTS AND DISCUSSION

During these rainfall measurements, all rainfall events have been recorded, with the maximum and minimum rainfall rates being 250 mm/h and 0.0058 mm/h, respectively, for the entire period of measurement. Then six different rainfall events with maximum rainfall intensities ranging between 10 mm/h and 40 mm/h for shower rainfall events and from 40 mm/h up to about 50 mm/h for

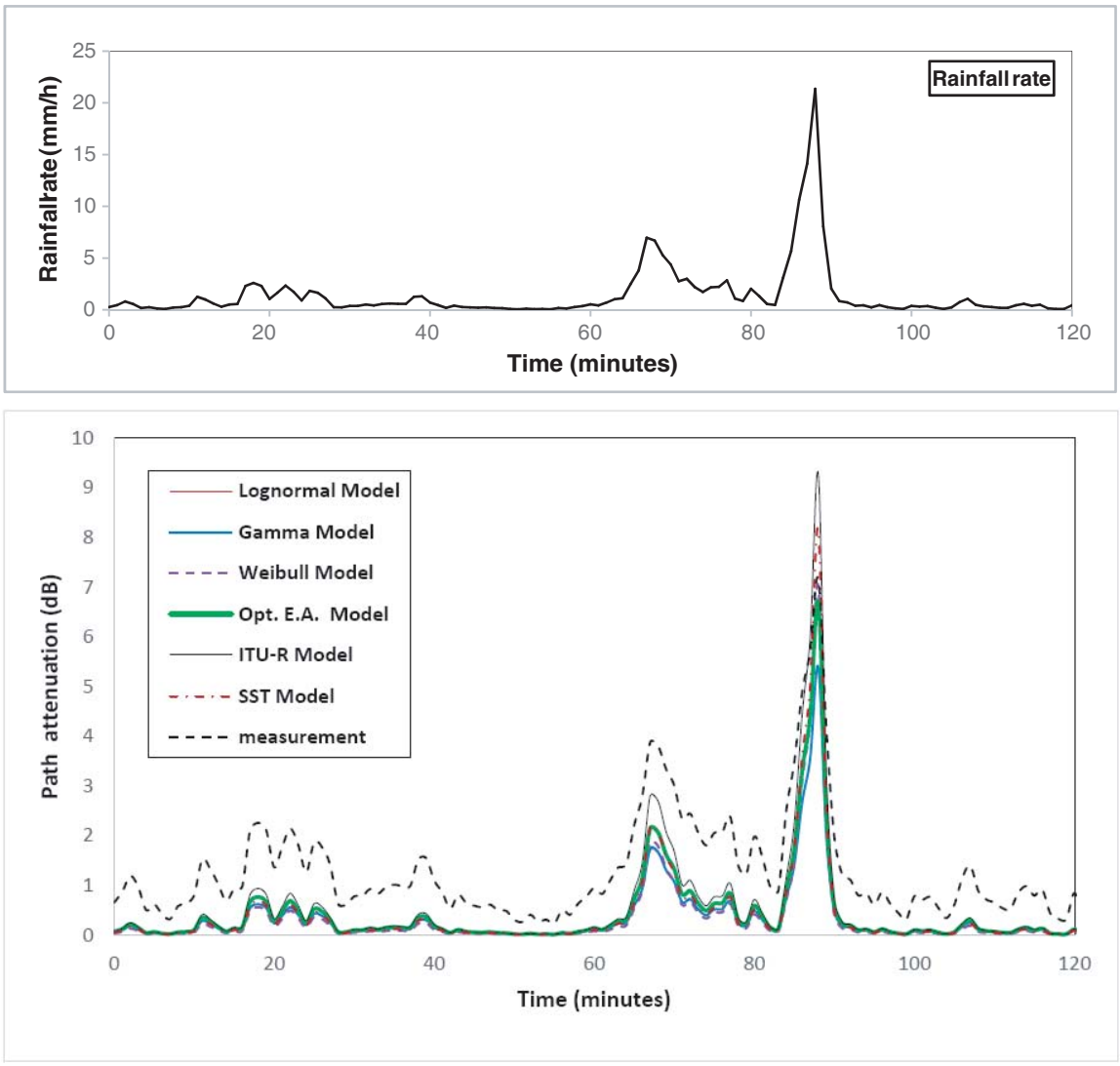

Figure 3. Time series of predicted and measured attenuation due to rain for event of 21/08/2014.

thunderstorm rainfall events recorded between 2014 and 2016 have been chosen and converted to rainfall attenuation time series using different attenuation prediction models presented in Section 3. For any given frequency and path length, these models can be used to calculate the predicted rainfall attenuation on any earth space link. Figures 3 to 8 present the comparison between the generated rainfall attenuation time series and the attenuation due to rain measured over the 12.6 GHz link for different rainfall events in Durban. As indicated earlier, the reason that we restrict our paper to rain rates up to 50 mm/h is that from experience with the satellite receiver, for rain rates higher than 50 mm/h, the receiver squelches, hence there would be no indication of "measured attenuation".

For the shower range (rain rates between 10–40 mm/h), we have 5 plots, with maximum rain rates at 21.3 mm/h, 23.69 mm/h, 27.81 mm/h, 32.2 mm/h, and 38.06 mm/h. For the thunderstorm regime, above 40 mm/h, we have a single plot, with peak rain rate at 45.02 mm/h. Figure 3 presents a comparison between the converted rainfall attenuation time series using different attenuation prediction models for a rainy event on 21/08/2014. As shown in the plot, the peak rainfall attenuation occurs when the corresponding rain rate is at the maximum. Note that what is of interest is the instantaneous attenuation rather than cumulative attenuation. We are thus focusing on the measured and estimated attenuation at the highest rain rate for any given rain event. In Figure 3, at the peak rain rate $R = 21.36$ mm/h,

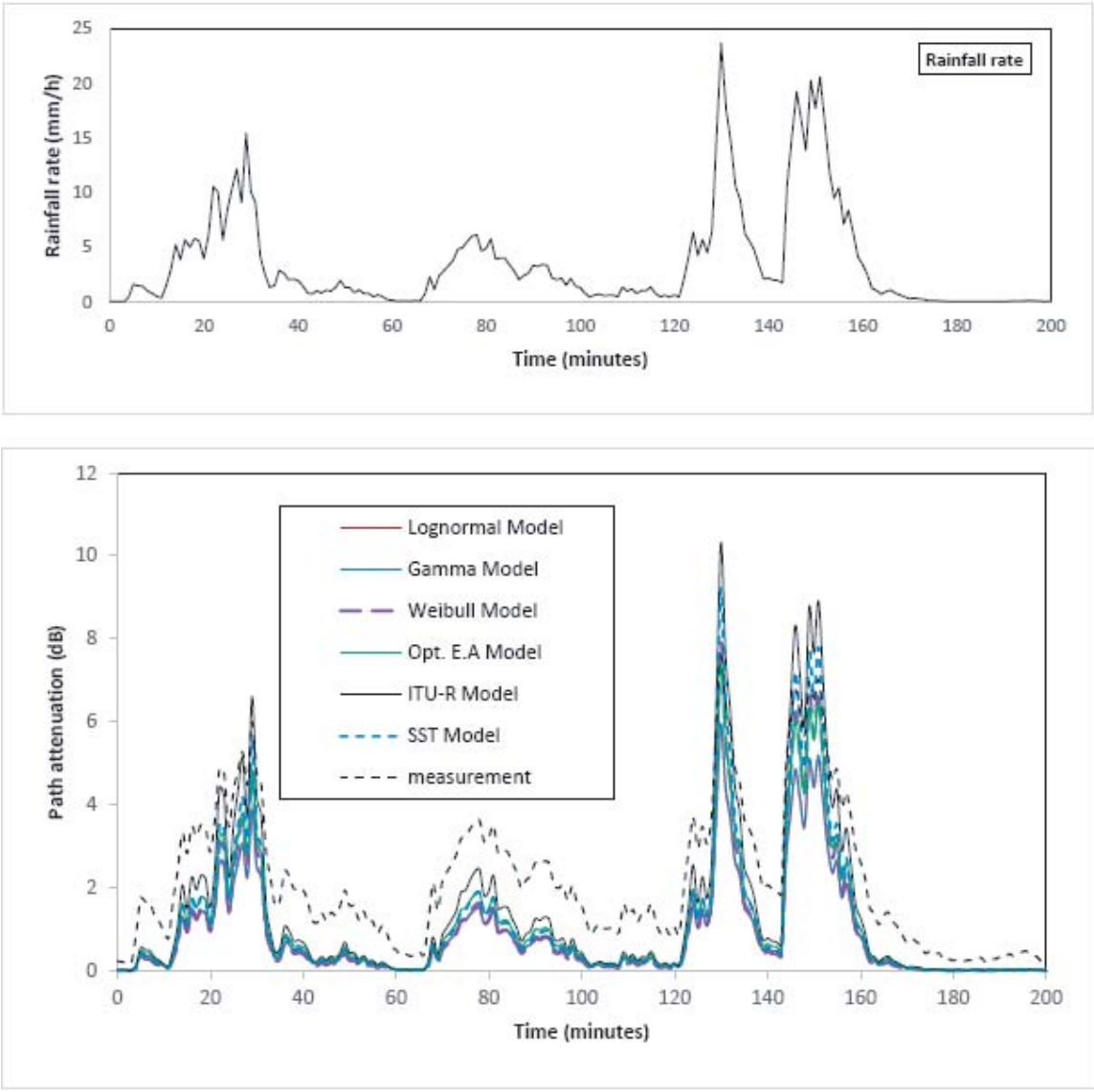

Figure 4. Time series of predicted and measured attenuation due to rain for event of 11/05/2014.

the corresponding attenuation peak values are: $A_{LGN} = 5.3\,\text{dB}$, $A_{GM} = 5.4\,\text{dB}$, $A_{WBL} = 7.0\,\text{dB}$, $A_{Opt\cdot E\cdot A} = 6.7\,\text{dB}$, $A_{ITU\text{-}R} = 9.3\,\text{dB}$, $A_{SST} = 8.1\,\text{dB}$ and the measured rain attenuation $A_m = 7.2\,\text{dB}$, which is closest to the prediction due to the Weibull attenuation model. Similarly, in Figure 4, the predicted and measured rain attenuation time series for a rainy event on 11/05/2014 are compared. As shown in the plot, at the peak rain rate $R = 23.69\,\text{mm/h}$, while the corresponding attenuation peak values are: $A_{LGN} = 5.9\,\text{dB}$, $A_{GM} = 6.0\,\text{dB}$, $A_{WBL} = 7.9\,\text{dB}$, $A_{Opt\cdot E\cdot A} = 7.3\,\text{dB}$, $A_{ITU\text{-}R} = 10.3\,\text{dB}$, $A_{SST} = 9.2\,\text{dB}$, and the measured rain attenuation $A_m = 7.6\,\text{dB}$ which is closest to the predictions due to the Optimised and Weibull attenuation models.

In Figure 5, the predicted and measured rain attenuation time series for a rainy event on 01/10/2014 are compared. As shown in the plot, at the peak rain rate, $R = 27.81\,\text{mm/h}$, while the corresponding attenuation peak values are: $A_{LGN} = 6.9\,\text{dB}$, $A_{GM} = 7.0\,\text{dB}$, $A_{WBL} = 9.5\,\text{dB}$, $A_{Opt\cdot E\cdot A} = 8.7\,\text{dB}$, $A_{ITU\text{-}R} = 12.2\,\text{dB}$, $A_{SST} = 11.1\,\text{dB}$, and the measured rain attenuation $A_m = 8.3\,\text{dB}$, which is closest to the value predicted by the Optimised attenuation model. In Figure 6, the predicted and measured rain attenuation time series for a rainy event on 07/05/2016 are compared. Again, as shown in the plot, at the

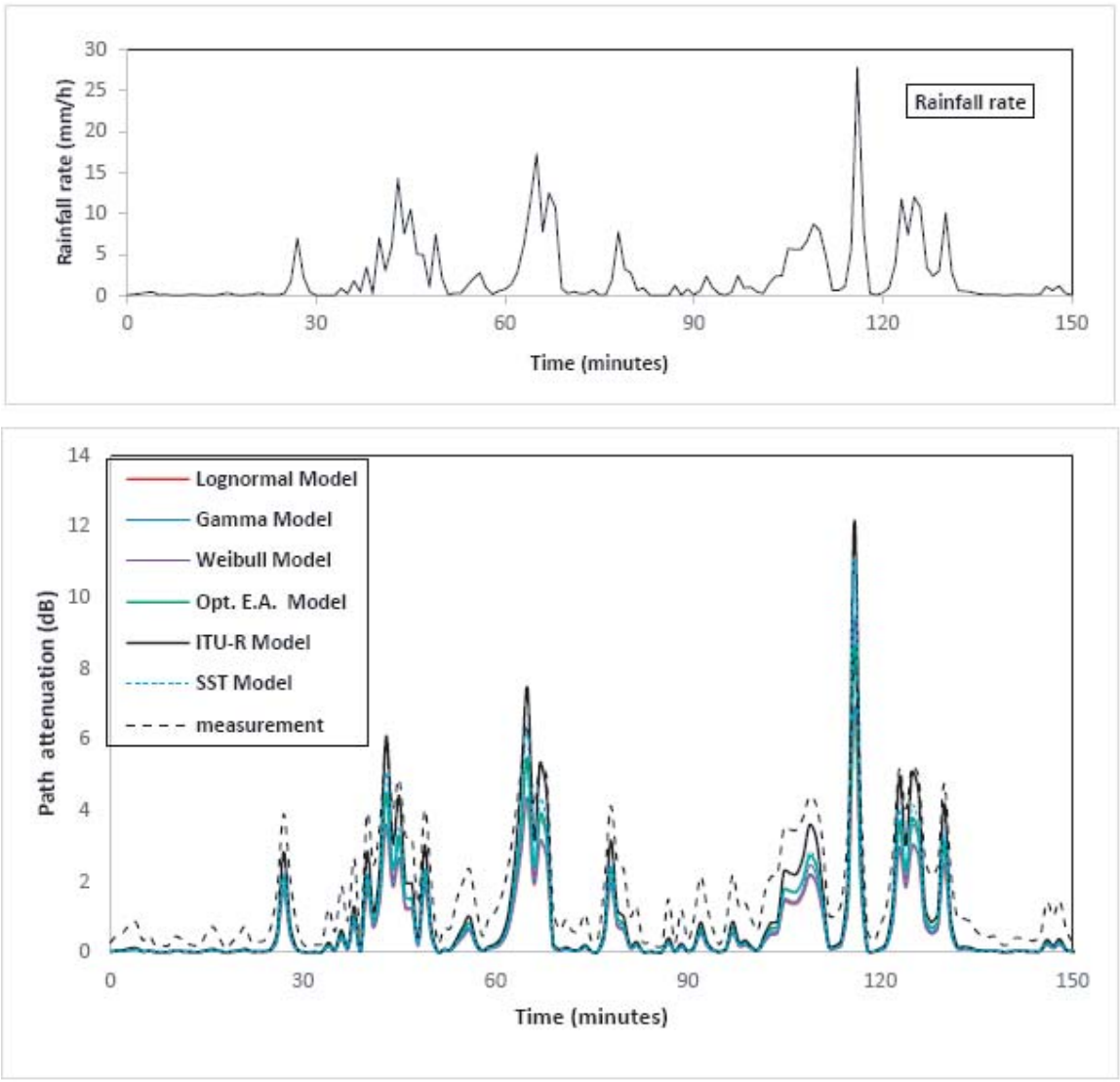

Figure 5. Time series of predicted and measured attenuation due to rain for event of 01/10/2014.

peak $R = 32.2\,\text{mm/h}$, the corresponding attenuation peak values are: $A_{LGN} = 7.9\,\text{dB}$, $A_{GM} = 8.0\,\text{dB}$, $A_{WBL} = 11.2\,\text{dB}$, $A_{Opt\cdot E\cdot A} = 10.0\,\text{dB}$, $A_{ITU\text{-}R} = 14.1\,\text{dB}$, $A_{SST} = 13.2\,\text{dB}$, with the measured rain attenuation $A_m = 8.98\,\text{dB}$, which is closest to the value predicted by the Optimised, Lognormal and Gamma models. In Figure 7, the predicted and measured rain attenuation time series for a rainy event on 07/05/2016 are compared. Again, at the peak rain rate of $R = 38.06\,\text{mm/h}$, the corresponding attenuation peak values are: $A_{LGN} = 9.32\,\text{dB}$, $A_{GM} = 9.45\,\text{dB}$, $A_{WBL} = 13.43\,\text{dB}$, $A_{Opt\cdot E\cdot A} = 11.71\,\text{dB}$, $A_{ITU\text{-}R} = 16.65\,\text{dB}$, $A_{SST} = 16.10\,\text{dB}$, and the measured rain attenuation $A_m = 9.84\,\text{dB}$, which is closest to the values predicted by both Lognormal and Gamma models. Finally, in Figure 8, the predicted and measured rain attenuation time series for a rainy event on 07/01/2016 are compared. At the peak rain rate $R = 45.02\,\text{mm/h}$, the corresponding attenuation peak values are: $A_{LGN} = 10.94\,\text{dB}$, $A_{GM} = 11.08\,\text{dB}$, $A_{WBL} = 16.14\,\text{dB}$, $A_{Opt\cdot E\cdot A} = 13.74\,\text{dB}$, $A_{ITU\text{-}R} = 19.65\,\text{dB}$, $A_{SST} = 19.63\,\text{dB}$, and the measured rain attenuation $A_m = 10.7\,\text{dB}$, which is closest to the value predicted by the Lognormal model.

Thus from the plots of Figures 3 to 8, results show that for a rainy event with low rain rate ($R < 10\,\text{mm/h}$), all rainfall attenuation predicted models underestimate the measured rainfall

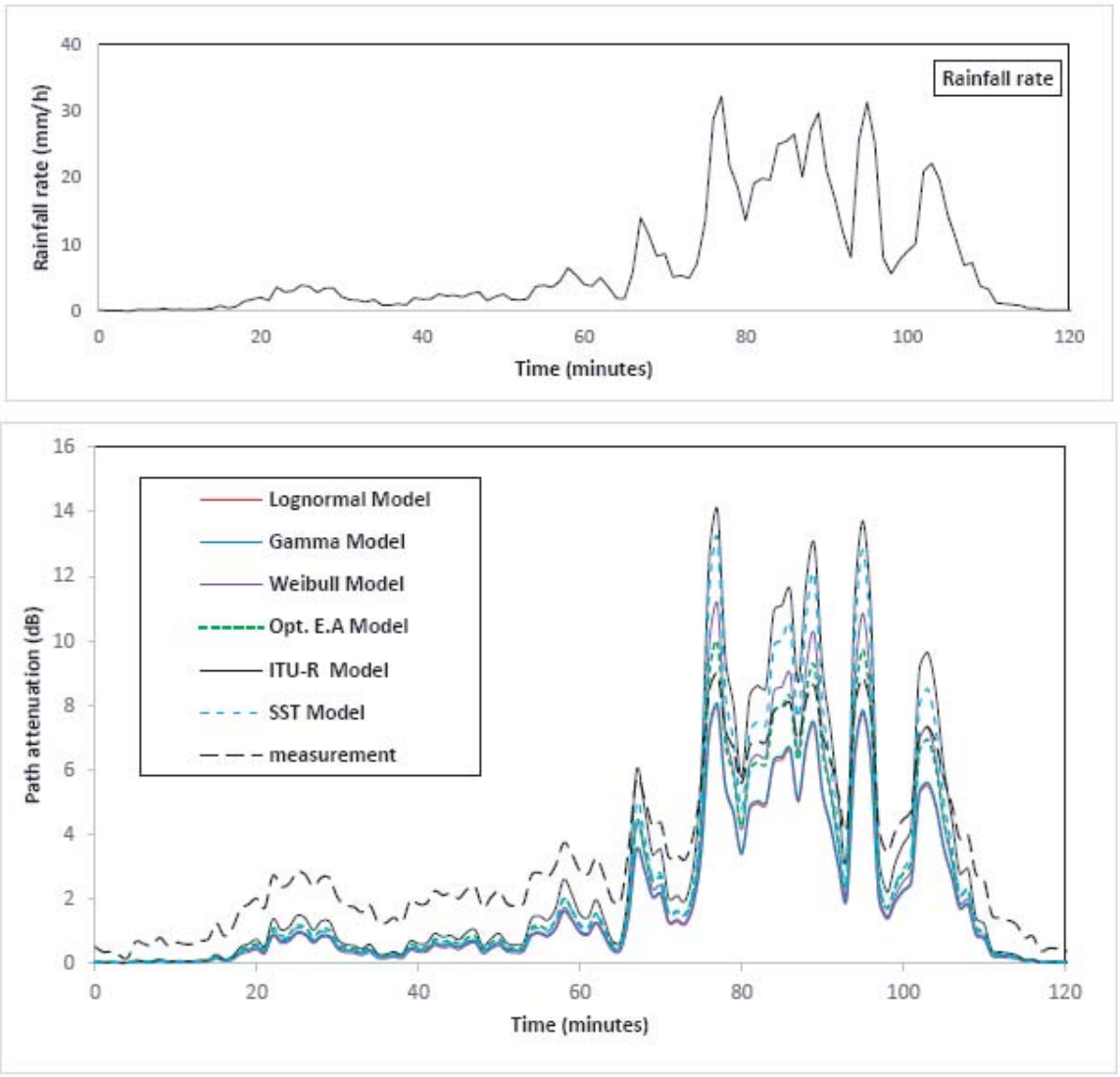

Figure 6. Time series of predicted and measured attenuation due to rain for event of 07/05/2016.

attenuation. In the range between 10 mm/h and 14 mm/h, the ITU-R prediction model predicts best as it returns the lowest percentage error among all considered models. Between 14 mm/h and 20 mm/h, the SST model performs better than the other considered models. Between 20 mm/h and 26 mm/h, both Optimised and Weibull models predict best as they return lower percentage errors than the other models. In the 26 mm/h to 34 mm/h range, the Optimized model predicts best as it returns the lowest percentage error among all considered models, while above 34 mm/h, both Lognormal and Gamma models are observed to predict best as they return lower percentage errors than the other presented models.

The percentage error (E) between the predicted path attenuation A_p (dB) and the measured path attenuation A_m (dB) is defined by [18]:

$$E = \frac{A_p - A_m}{A_m} \times 100\% \tag{39}$$

where A_m (dB) is the measured path attenuation, and A_p (dB) is the predicted path attenuation.

From Table 5, from the first row at 10 mm/h and the second at 15 mm/h, it is seen that the ITU-R model best fits the measurement with lowest percentage error value among all the models. At

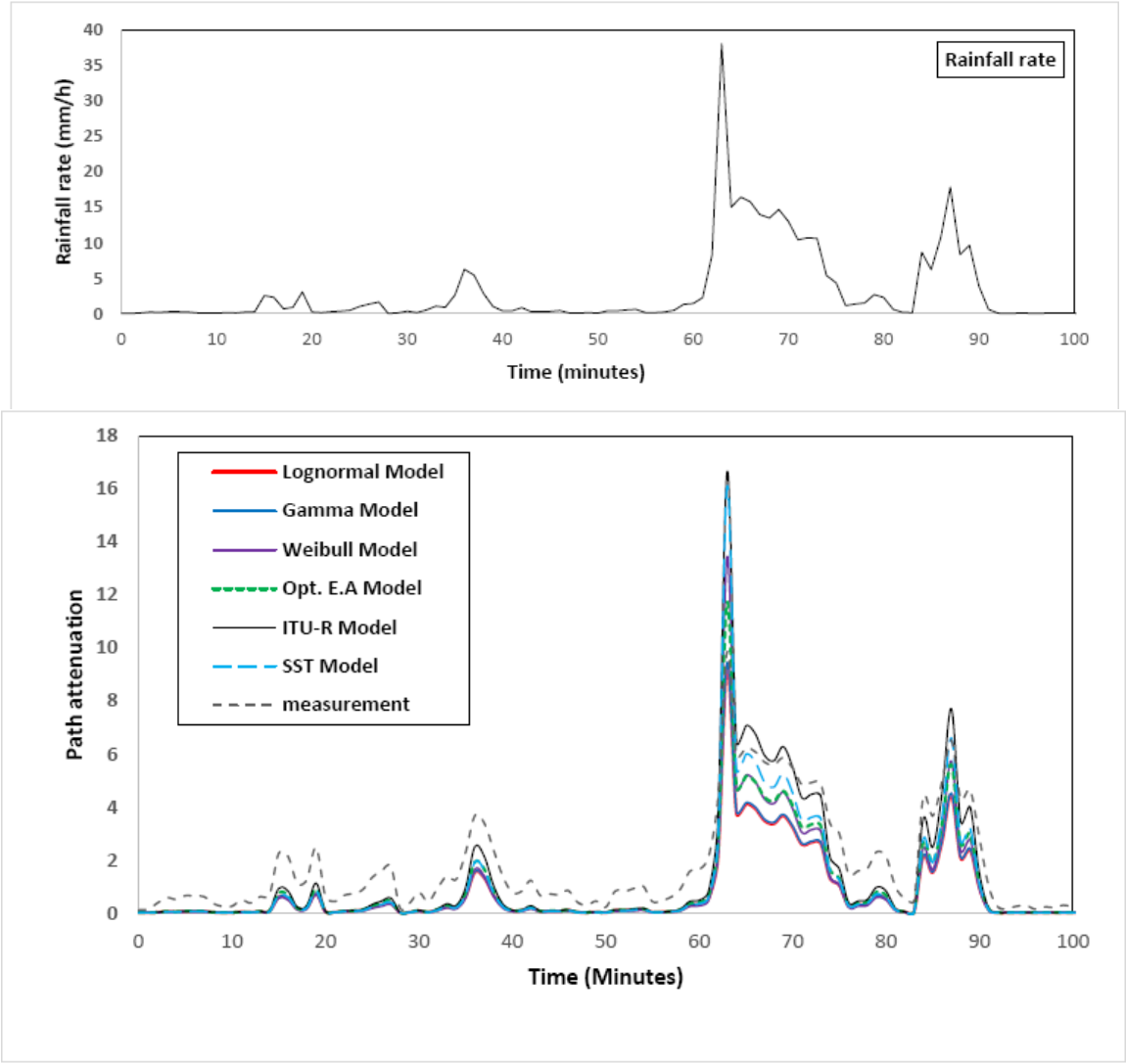

Figure 7. Time series of predicted and measured attenuation due to rain for event of 04/04/2014.

Table 5. Comparison between measured and predicted rainfall attenuation models.

R (mm/h)	A_m (dB)	A_{LGN} (dB)	Error (%)	A_{GM} (dB)	Error (%)	A_{WBL} (dB)	Error (%)	A_{Opt} (dB)	Error (%)	A_{ITU} (dB)	Error (%)	A_{SST} (dB)	Error (%)
10	4.73	2.5	46.8	2.5	46.8	2.9	38.9	3.1	34.2	4.2	12.1	3.3	29.5
15	5.91	3.7	36.8	3.8	35.8	4.7	21.1	4.7	20.5	6.4	8.5	5.4	9.1
20	6.92	5.0	28.1	5.1	27.0	6.5	5.9	6.3	9.5	8.7	25.3	7.5	9.0
25	7.82	6.2	20.7	6.3	19.5	8.4	7.5	7.8	0.2	10.9	39.5	9.8	25.5
30	8.64	7.4	14.2	7.5	13.0	10.3	19.4	9.3	7.9	13.1	51.9	12.2	40.8
35	9.40	8.6	8.5	8.7	7.3	12.2	30.3	10.8	15.0	15.3	63.0	14.6	55.2
40	10.11	9.8	3.5	9.9	2.1	14.2	40.3	12.3	21.4	17.5	72.97	17.1	68.8
45	10.79	10.9	1.4	11.1	2.7	16.1	49.5	13.7	27.3	19.6	82.1	19.6	81.9

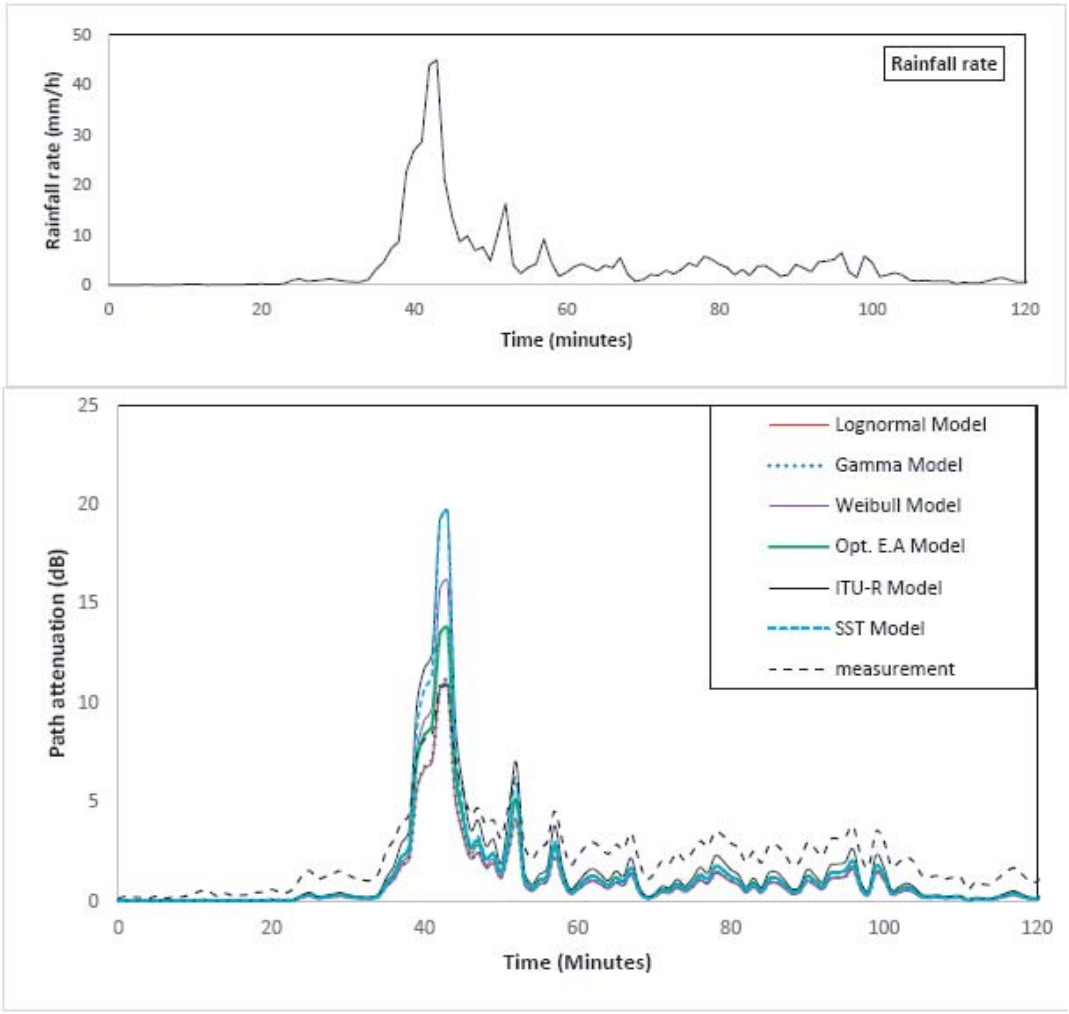

Figure 8. Time series of predicted and measured attenuation due to rain for event of 07/01/2016.

20 mm/h, it is seen that the Weibull model predicts better as it returns lower percentage error than other considered models. At 25 mm/h and 30 mm/h, results show that the Optimized model predicts the measured attenuation better than the other models. At 35 mm/h, the Gamma attenuation model provides the best prediction, while At 40 mm/h and 45 mm/h, the Lognormal and Gamma models perform best, as they give the lowest percentage error values among all presented models. For example, at 35 mm/h, the difference between the measured attenuation and the predicted attenuation corresponds to the following percentage errors: 8.5%, 7.3%, 30.3%, 15.0%, 63.0% and 55.2%, for the LGN, GM, WBL, Opt. EA, ITU-R, and SST models, respectively. For $R = 40$ mm/h, the difference between the measured attenuation and predicted attenuation values corresponds to the following percentage errors: 3.5%, 2.1%, 40.3%, 21.4%, 73.0%, and 68.8% for the LGN, GM, WBL, Opt. EA, ITU-R, and SST models, respectively. Finally, for $R = 45$ mm/h the difference between the measured attenuation and predicted attenuation values corresponds to the following percentage errors: 1.4%, 2.7%, 49.5%, 27.3%, 82.1%, and 81.9% for the LGN, GM, WBL, Opt. EA, ITU-R, and SST models, respectively.

Averaging the percentage error for the eight sampled rain rates from 10 mm/h to 45 mm/h, it is seen that the "Optimized" model presents the lowest average error of 17.7%, followed by the Gamma model with an average error of 19.3%, the Lognormal model with an average error of 20.0%, the Weibull model with 26.6%, the SST model with 40.0%, and the ITU-R model with 44.4%. These are plotted in Figures 9 and 10, where we note that the Lognormal and Gamma models have almost identical error trends, with their lowest error at the higher rain rates above 35 mm/h. On the other hand, the

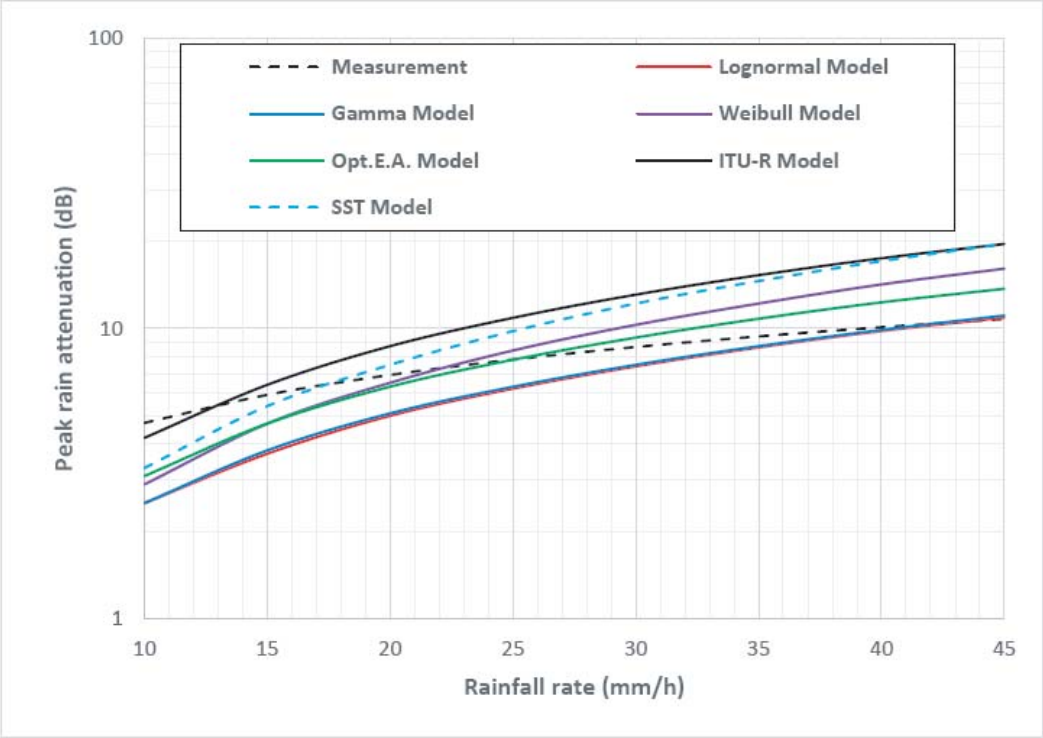

Figure 9. Measured and predicted rain attenuation at peak rain rate.

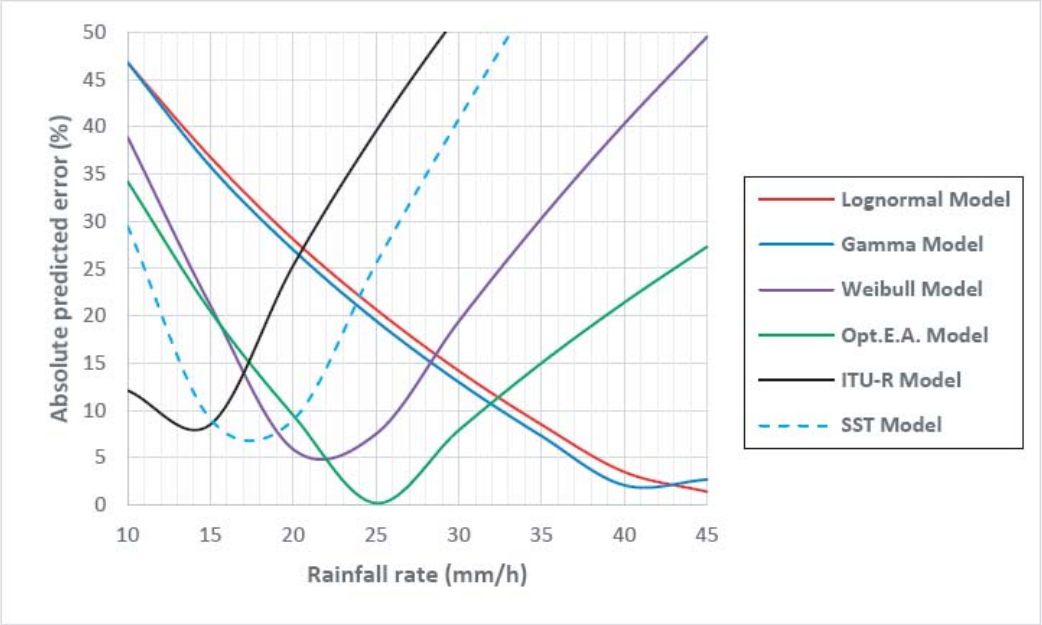

Figure 10. Percentage error between measurement and prediction at various rain-rate peaks.

"Optimized" and Weibull models tend to reduce the errors for both lower rain rates (widespread and shower) and the thunderstorms.

The cumulative distribution of rainfall attenuation over three years between 2014 and 2016 in Durban is plotted in Figure 11. From Figure 11, as per ITU-R recommendation, to get 99.99%

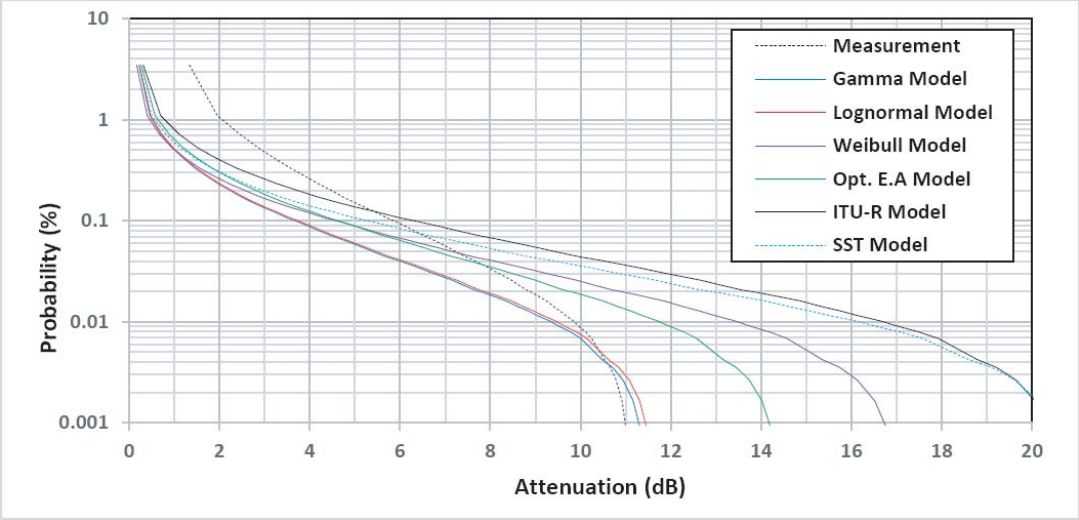

Figure 11. Rainfall attenuation exceedence probability in Durban averaged over three years, 2014–2016.

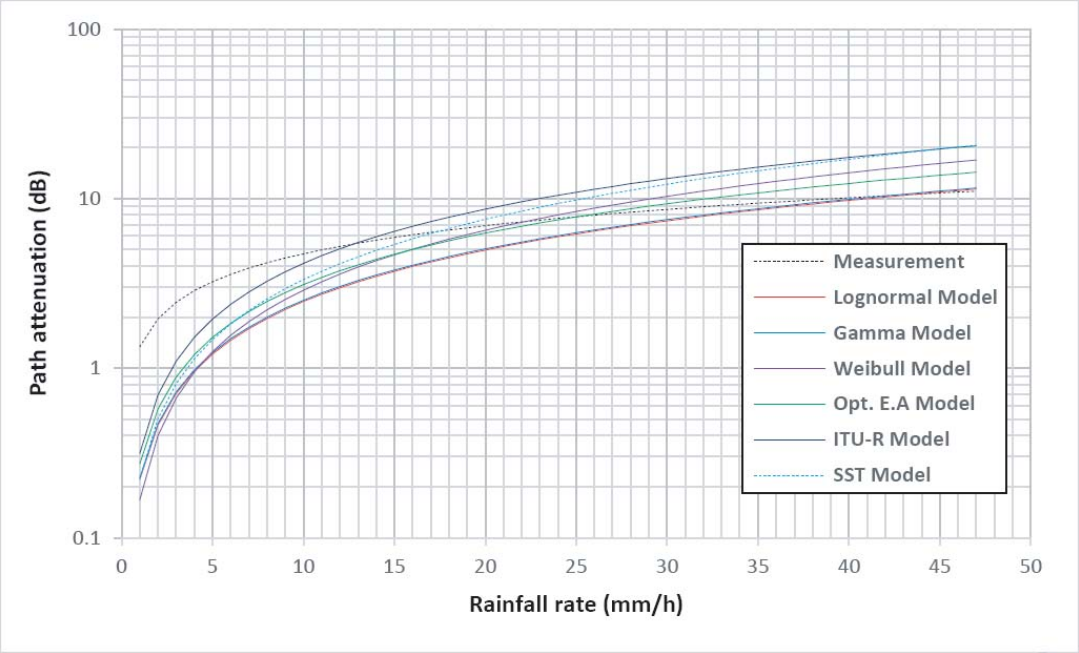

Figure 12. Comparison between measured rainfall attenuation and predicted rainfall attenuation Models.

availability, the estimated fade margin varies between 9.4 dB and 17.1 dB, where the measured rainfall attenuation is 9.9 dB, which is closest to the Lognormal prediction at this point. Figure 12 presents a comparison between measured rainfall attenuation and those converted by different rainfall attenuation models. From these plots, one observes that these attenuation prediction models have varying performances as the rainfall rate increases.

For the overall performance of the link, all the proposed attenuation models are tested up to

Table 6. Error estimation from different attenuation models.

Rain rate (mm/h)	LGN	GM	WBL	Opt. EA	ITU-R	A (SST)
$10 \leq R < 40$	1.654	1.581	1.857	1.114	3.832	3.223
$40 \leq R < 50$	0.622	0.712	5.617	3.202	9.105	9.137

50 mm/h rainfall rate using the root mean square error (RMSE). The RMSE test is given by [18]:

$$RMSE = \sqrt{\frac{1}{n}\sum_{i=1}^{n}[f^* - f]^2} \tag{40}$$

where f^* is the measured attenuation and f the predicted attenuation and n the sample size.

Using Equation (39), the evaluated results are presented in Table 6. From this table, the "Optimized" attenuation prediction model best fits with RMSE of 1.114 for the rainfall events with rain intensities between 10 mm/h and 40 mm/h. Between 40 mm/h and about 50 mm/h, the Lognormal attenuation prediction model best fits the measurement with the lowest RMSE value of 0.622 compared to the other models.

5. CONCLUSION

In this paper, the ITU-R model, Synthetic Storm Technique, and other raindrop size distribution models are used to generate rainfall attenuation time series from rainfall rate measurements collected in Howard College, University of Kwa-Zulu Natal. Error analysis based on comparisons between predicted rainfall attenuation models and measured rainfall attenuation at 12.6 GHz satellite TV link shows that the "Optimized" and Lognormal attenuation prediction models best predict the attenuation, as they give the closest results to the measurement. Indeed, for the shower regime (up to 40 mm/h), the Optimized model gives the best estimate of attenuation due to rain in South Africa, while for the thunderstorm range (rain rates above 40 mm/h), the Lognormal attenuation model (closely followed by the Gamma model) is recommended for prediction in order to implement fade mitigation over Ku-band Satellite links in South Africa.

REFERENCES

1. Matricciani, E., "Time diversity as a rain attenuation countermeasure in satellite links in the 10–100 GHz frequency bands," *2006 First European Conference on Antennas and Propagation*, 1–6, IEEE, 2006.
2. Nakajo, R. and Y. Maekawa, "Characteristics of rain attenuation time variation in Ka band satellite communications for the kind of rain types in each season," *2012 International Symposium on Antennas and Propagation (ISAP)*, 1473–1476, IEEE, 2012.
3. Afullo, T. J. O., "Raindrop size distribution modeling for radio link design along the eastern coast of South Africa," *Progress In Electromagnetics Research B*, Vol. 34, 345–366, 2011.
4. Akuon, P. O. and T. J. O. Afullo, "Rain cell sizing for the design of high capacity radio link systems in South Africa," *Progress In Electromagnetics Research B*, Vol. 35, 263–285, 2011.
5. Alonge, A. A. and T. J. O. Afullo, "Rainfall microstructural analysis for microwave link networks: Comparison at equatorial and subtropical Africa," *Progress In Electromagnetics Research B*, Vol. 59, 45–58, 2014.
6. Adetan, O. E. and T. J. Afullo, "Raindrop size distribution and rainfall attenuation modeling in equatorial subtropical Africa: Critical diameters," *Annals des Telecommunication*, 1–13, 10.1007/s12243-013-0418-z, 2014.
7. Sumbiri, D., T. J. O. Afullo, and A. A. Alonge, "Rainfall zoning and rain attenuation mapping for microwave and millimetric applications in central Africa," *International Journal on Communications Antenna and Propagation (IRECAP)*, Vol. 6, No. 4, 198–210, 2016.

8. Afolayan, B. O., T. J. Afullo, and A. Alonge, "Subtropical rain attenuation statistics on 12.6 GHz ku-band satellite link using Synthetic Storm Technique," *SAIEE Africa Research Journal*, Vol. 109, No. 4, 230–236, December 2018.
9. Ahuna, M. N., T. J. Afullo, and A. A. Alonge, "30-second and one-minute rainfall rate modelling and conversion for millimetric wave propagation in South Africa," *SAIEE Africa Research Journal*, Vol. 107, No. 4, 17–29, March 2016.
10. Afolayan, B., T. Afullo, and A. Alonge, "Seasonal and annual analysis of slant path attenuation over a 12 GHz earth-satellite link in subtropical Africa," *International Journal on Communications Antenna and Propagation (IRECAP)*, Vol. 7, No. 7, 572–580, 2017.
11. Ahuna, M. N., T. J. O. Afullo, and A. Alonge, "Outage prediction during intense rainstorm events using queuing theory and Markov Chains over radio links," *Progress In Electromagnetics Research M*, Vol. 73, 183–196, 2018.
12. Alonge, A. A., "Semi-empirical characteristics of modified lognormal DSD inputs using rain rate distributions for radio links over the African Continent," *Advances in Space Research*, Vol. 67, No. 1, 179–197, 2021.
13. Ajayi, G. O. and R. L. Olsen, "Modelling of a raindrop size distribution for microwave and millimetre wave applications," *Radio Science*, Vol. 20, No. 2, 193–202, 1985.
14. Adimula, I. and G. Ajayi, "Variation in raindrop size distribution and specific attenuation due to rain in Nigeria," *Ann. Telecom.*, Vol. 51, No. 1–2, 87–93, 1996.
15. Adetan, O. and T. J. Afullo, "Three-parameter raindrop size distribution modeling for microwave propagation in South Africa," *Proceedings of the International Association of Science and Technology for Development (IASTED), International Conference on Modeling and Simulation (Africa MS 2012)*, 155–160, 2012.
16. Sekine, M. and G. Lind, "Rain attenuation of centimeter, millimeter and submillimeter radio waves," *Proc. of 12th European Microwave Conference*, 584–589, 1982.
17. Jiang, H., M. Sano, and M. Sekine, "Weibull raindrop-size distribution and its application to rain attenuation," *IEE Proc. Microw. Antennas Propag.*, Vol. 144, No. 3, 197–200, June 1997.
18. Sumbiri, D. and T. J. O. Afullo, "Optimized rain drop size distribution model for microwave propagation for equatorial Africa," *SAIEE Africa Research Journal*, Vol. 111, No. 1, 22–35, March 2020.
19. ITU-R, "Propagation data and prediction methods required for the design of Earth-space telecommunication systems," *Recommendation ITU-R*, 618-13, 2017.
20. ITU-R, "Rain height model for prediction methods," *Recommendation ITU-R*, 839-4, 2013.
21. ITU-R, "Specific attenuation model for rain for use in prediction methods," *ITU-R P.838-3*, Geneva, 1992–1999–2003–2005.
22. Freeman, R. L., *Radio System Design for Telecommunications*, John Wiley and Sons, New York, 2007.
23. Olsen, R. L, D. V. Rogers, and D. B. Hodge, 1978, "The aR^b relation in the calculation of rain attenuation," *IEEE Trans. Antennas & Propag.*, Vol. 26, No. 2, 318–329, March 1978.
24. Drufuca, G., "Rain attenuation statistics for frequencies above 10-GHz from rain gauge observations," *J. Res. Atmosphere*, Vol. 8, No. 1, 2, 399–411, 1974.
25. Bertok, E., G. D. Renzis, and G. Drufuca, "Estimate of attenuation due to rain at 11-GHz from rain gauge data," *URSI Commission F Open Symposium*, La Baule, 1997, 295–300.
26. Matricciani, E., C. Riva, and L. Castanet, "Performance of the synthetic storm technique in a low elevation 5 slant path at 44.5 GHz in the French Pyrénées," *Proc. First European Conference on Antennas and Propagation (EuCAP)*, 1–6, 2006.
27. Kourogiorgas, C. I., A. D. Panagopoulos, J. D. Kanellopoulos, S. N. Livieratos, and G. E. Chatzarakis, "Investigation of rain fade dynamic properties using simulated rain attenuation data with synthetic storm technique," *Proc. 7th European Conference on Antennas and Propagation (EuCAP)*, 2277–2281, 2013.

28. Sánchez-Lago, I., F. Fontán, P. Mariño, and U.-C. Fiebig, "Validation of the synthetic storm technique as part of a time-series generator for satellite links," *IEEE Antennas and Wireless Propagation Letters*, Vol. 6, 372–375, October 2007.
29. Lwas, A. K., Md. R. Islam, J. Chebil, M. H. Habaebi, A. F. Ismael, A. Zyoud, and H. Dao, "Rain attenuation analysis using Synthetic Storm Technique in Malaysia," *IOP Conference Series: Materials Science and Engineering*, Vol. 53, No. 1, 012045, 2013.
30. Matricciani, E., "Physical-mathematical model of the dynamics of rain attenuation based on rate time series and a two-layer vertical structure of precipitation," *Radio Sci.*, Vol. 31, No. 02, 281–295, March–April 1996.
31. Maggiori, D., "The computed transmission through rain in the 1–400 GHz frequency range for spherical and elliptical drops at any polarisation," *Alta Freq.*, No. 50, 262–273, 1981.
32. Jiang, H., M. Sano, and M. Sekine, "Weibull raindrop-size distribution and its application to rain attenuation," *IEE Proc. Microw. Antennas Propag.*, Vol. 144, No. 3, 197–200, June 1997.
33. Maitra, A., S. Das, and A. K. Shukla, "Joint statistics of rain rate and event duration for a tropical in India," *Indian Journal of Radio & Space Physics*, Vol. 38, No. 6, 353–360, January 2010.
34. Malinga, S. J. and P. A. Owolawi, "Obtaining raindrop size model using the method of moments and its applications for South African radio systems," *Progress In Electromagnetics Research B*, Vol. 46, 119–138, 2013.
35. Ajayi, G. O., S. Feng, S. M. Radicella, B. M. Reddy (eds.), *Handbook on Radiopropagation Related to Satellite Communications in Tropical and Subtropical Countries*, ICTP, Trieste, Italy, 1996.
36. Alonge, A. A., "Correlation of rain dropsize distribution with rain rate derived from disdrometers and rain gauge networks in Southern Africa," MSc. Thesis, University of Kwa-Zulu Natal, December 2011.
37. Sumbiri, D., "Microwave and millimetre radio wave propagation modelling for terrestrial line-of-sight links in Central Africa," Ph.D. Thesis, University of Kwa-Zulu Natal, June 2018.